# Ultrafast-electron dynamics and recombination on the Ge(111)(2×1) $\pi$-bonded surface

R. Haight and M. Baeumler*
*IBM Thomas J. Watson Research Center, P.O. Box 218, Yorktown Heights, New York 10598*
(Received 14 November 1991)

Angle-resolved laser-photoemission spectroscopy has been used to study the ultrafast-electron scattering and recombination processes on the Ge(111) $\pi$-bonded (2×1) surface with subpicosecond time resolution. Electrons photoexcited into the bulk Ge conduction band scatter into the unoccupied surface antibonding $\pi^*$ band whose minimum is at the $\bar{J}$ point in the surface Brillouin zone. Rapid relaxation to the surface-band minimum is followed by a unique phonon-assisted process in which electrons recombine with bulk holes at the valence-band maximum, which we find to be the primary mechanism responsible for the decay of the transient $\pi^*$ population. Time-dependent measurements carried out at 300 and 120 K have been employed to determine the role of energetic phonons in the scattering processes. These processes are modeled with a set of rate equations, whose fits to the data yield scattering times used to determine a surface recombination velocity directly. Ultrafast surface-state hole dynamics are observed, and a renormalization of the surface band gap is studied as a function of electron density. The $\pi$-bonded states are fundamentally one dimensional in nature, and thus these results represent studies of band-gap renormalization in a one-dimensional system.

## I. INTRODUCTION

Elucidation of the microscopic processes involved in ultrafast-electron dynamics is critical to the understanding of macroscopic transport in semiconductor systems. Processes including electron-phonon (*e*-ph), electron-electron, and electron-impurity scattering, as well as electron-hole (*e*-*h*) recombination are just a few of the mechanisms which must be considered. In a semiconductor heterostructure system, for example, an electron which crosses the interface between the two materials will scatter from the band minimum of the substrate to a new band in the overlayer. The details of such scattering can conceivably be extremely complex when, for example, lattice mismatch, interfacial disorder, and interdiffusion are included. A somewhat simpler system, in which many ingredients of this problem can be found, is the surface of a semiconductor, where reconstruction of the surface atoms results in new states which are often considerably different from those of the bulk.

A particularly interesting system for studying many aspects of the aforementioned electron dynamics is the cleaved Ge(111)(2×1) surface, where the surface atomic rearrangement gives rise to $\pi$-bonded chains of atoms oriented along the $[01\bar{1}]$ direction (Fig. 1, top) separated by 8 Å along the $[2\bar{1}\,\bar{1}]$ direction. Both Ge(111) and Si(111) exhibit similar reconstructions and surface energy-band structures, and represent among the most intensively studied and best understood (theoretically and experimentally) semiconductor surface systems to date.[1–5] This level of understanding provides a foundation for investigating the ultrafast excited-state dynamics on these surfaces. In the particular case of Ge, the atomic chains which form upon cleavage give rise to new electronic states at the surface, which are energetically located within the bulk band gap of the crystal. Figure 1 (bottom) displays the surface and bulk projected band struc-

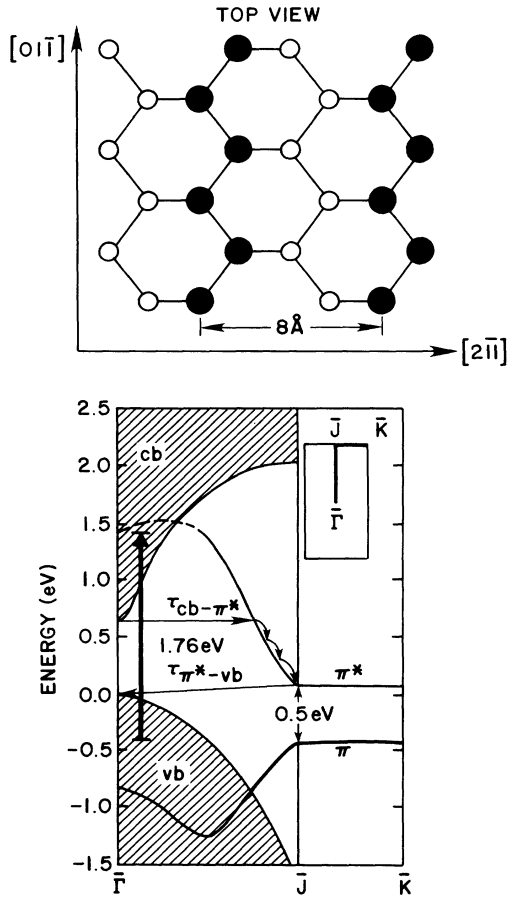


FIG. 1. Top view of the $\pi$-bonded chains formed at the cleaved Ge(111) surface. The $\pi$-bonded surface atoms are shown as filled circles (top). Bulk projected and surface band structure of the cleaved Ge(111)(2×1) $\pi$-bonded surface. The excitation, scattering, and recombination pathways are depicted by arrows. The inset shows the surface Brillouin zone (bottom).

 ©1992 The American Physical Society

ture for this particular reconstruction. For Ge, the conduction-band minimum (CBM) is the $L$ point, 0.66 eV above the valence-band maximum (VBM), and when projected onto the surface along the [111] direction defines the minimum unoccupied point at $\bar{\Gamma}$, the surface Brillouin zone (SBZ) center. The bulk conduction band at the $\Gamma$ point (also at $\bar{\Gamma}$) is 0.9 eV above the VBM. The solid curves represent the surface bands. These surface bonding and antibonding bands disperse upward (occupied $\pi$) and downward (unoccupied $\pi^*$) along the $[01\bar{1}]$ direction until they reach the $\bar{J}$ point of the SBZ. The bands are nearly dispersionless along the perpendicular $[2\bar{1}\,\bar{1}]$ direction, mirroring the one-dimensional nature of the chains (see Fig. 1). As a result, strong optical absorption, $\sim 2\%$, has been observed for photons at the surface band-gap energy of 0.5 eV.[6] In this paper, we will describe in detail the manner in which electrons, initially excited into bulk Ge bands, couple into surface states, lose energy, and eventually recombine with holes also present at the surface.[7] We expect that the scattering and recombination mechanisms observed in our experiments will be operative in a wide class of heterostructure semiconductor systems.

## II. EXPERIMENTAL DETAILS

Our laser-photoemission studies were carried out as a series of excite-probe experiments where electrons are first excited into empty states above the Fermi level (excite pulse), and subsequently photoemitted (probe pulse). Since both photon pulses are derived from the same laser source, temporal synchronization is obtained. The laser photoemission technique has been described in detail elsewhere,[8] but a brief outline will be given here. A dye laser, synchronously pumped by a Nd:YAG (yttrium-aluminum-garnet) laser produces 0.8-ps pulses of light, tuned for this experiment to 704 nm (1.76 eV). Pulses from this laser are amplified at a 100-Hz repetition rate in a four-stage XeCl excimer-pumped amplifier, yielding $\sim 0.4$ mJ per pulse. A fraction of this light is frequency doubled to 352 nm (3.52 eV) in a nonlinear crystal (potassium dihydrogen phosphate) and then subsequently frequency tripled in a Xe conversion cell. The resulting 117.3-nm (10.56-eV) radiation is selected by a spherical grating and focused onto the sample. Unconverted 1.76-eV light is used to photoexcite the sample and impinges on the surface colinearly with the 10.56-eV light in order to avoid geometrical broadening of the time resolution. The 1.76-eV flux was varied between 90 and 800 $\mu J/cm^2$, resulting in a peak bulk carrier density of $(1-9)\times 10^{19}/cm^3$ at the surface. The highest fluences used were still three orders of magnitude below the melting threshold, and no significant heating of the sample was observed. Photoemitted electrons were energy and angle analyzed with a 64-anode time-of-flight detector, with an energy resolution of $<0.1$ eV for electrons with 6-eV kinetic energy. The acceptance angle of 3.8° provides a momentum resolution of 0.07 $\text{Å}^{-1}$ at the $\bar{J}$ point.

Samples of both $n$- and $p$-type doping were cleaved *in situ* along the $[2\bar{1}\,\bar{1}]$ direction, and could be cooled to 120 K in order to investigate temperature-dependent phenomena. A six-axis manipulator was employed to permit detection of photoemitted electrons from all energetically accessible points in the bulk or surface Brillouin zone. The cleaved surfaces were inspected with low-energy electron diffraction, and used only if they exhibited the desired single-domain $(2\times 1)$ reconstruction. The ultrahigh-vacuum system attains a base pressure of $5\times 10^{-11}$ Torr, which is critical since the $(2\times 1)$ reconstruction of this surface is metastable and photoemission intensities of the surface states are sensitive to residual gas contamination.

## III. SPECTROSCOPY

Upon photoexcitation of the system, a significant population of electrons ($\sim 5\times 10^{19}/cm^3$ at the surface) is created by absorption in the bulk. Inspection of the Ge-bulk band structure,[9] displayed in Fig. 2, shows that absorption of 1.76-eV photons occurs near the bulk-$\Gamma$ point only. Holes are created 0.4 eV below the VBM, while electrons are excited 0.5 eV above the conduction edge near $\Gamma$. Electrons can relax to the band edge at $\Gamma$, as well as scatter rapidly to the CBM at $L$, which possesses a large density of states. Since bulk and surface states overlap at the surface, electrons may also scatter into the $\pi^*$ band, $\sim 0.4$ eV above the $\pi^*$ minimum at the surface $\bar{J}$ point, and eventually relax to the band minimum (Fig. 1, bottom). Figure 3 displays a photoemission spectrum of the $2\times 1$ surface collected at 120 K, and an emission angle of 39° along the $[01\bar{1}]$ (chain) direction, when the probe pulse was delayed 5 ps relative to the excite pulse. We observe two intense peaks, one at 0 eV on our energy scale and another at 0.5 eV. A study of the intensity dependence of the 0.5-eV peak with emission angle (see Fig. 4), collected along the $\bar{\Gamma}$-$\bar{J}$ (chain) direction, reveals that the center of the distribution occurred at 39° relative to the sample normal, indicating a peak in the concentration of electrons at this point in the SBZ. With this infor-

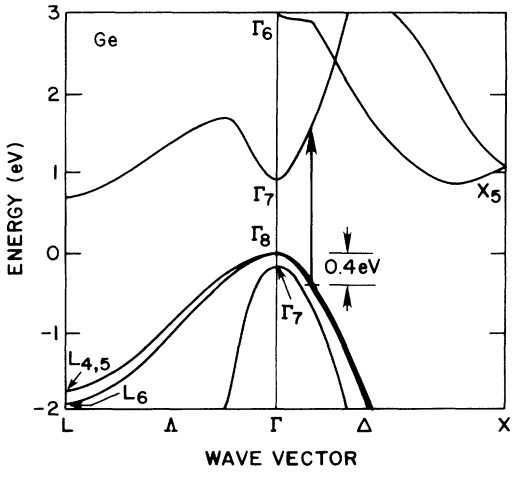


FIG. 2. Band structure of bulk Ge (after Ref. 8) indicating a point in the Brillouin zone where absorption of the 1.76-eV excitation pulse occurs. Holes are created 0.4 eV below the VBM, which can scatter into the $\pi$ band. Absorption also occurs along the $\Lambda$ direction (not shown).

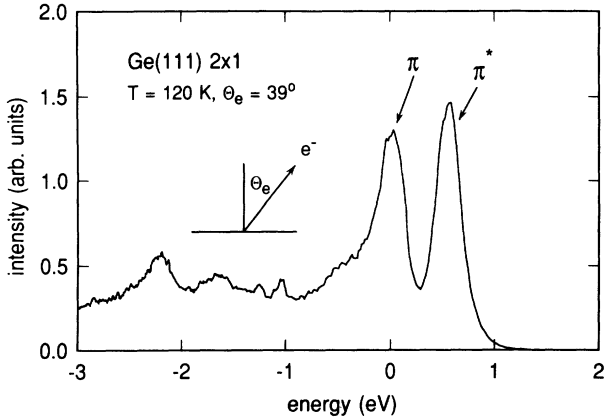


FIG. 3. Excite-probe spectrum of the Ge(111)(2×1) surface, collected at 120 K, and an emission angle of 39°. The probe pulse was delayed 5 ps relative to the excite pulse.

mation, we can calculate the parallel component of the electron wave vector, $k_{\parallel}$, for an emission angle 39° and our photon energy of 10.56 eV. Because $k_{\parallel}$ is a good quantum number for the surface, and is conserved in the photoemission process, modulo a reciprocal-lattice vector, we calculate $k_{\parallel}=[(2m_eE_{\rm kin}/\hbar^2)]^{1/2}\sin(39°)=0.786$ Å$^{-1}$, where $m_e$ is the electron mass and $E_{\rm kin}=6.0$ eV, the kinetic energy of a photoemitted $\pi^*$ electron measured in our analyzer. This value of $k_{\parallel}$ corresponds to the $\bar{J}$ point in the SBZ, and we therefore assign the 0-eV peak to the normally occupied $\pi$ state, and the 0.5-eV emission to the now transiently occupied $\pi^*$ band. The 0.5-eV separation is in good agreement with optical-absorption measurements on this surface.[6] We note at this point that the $\pi^*$ peak is slightly more intense than the $\pi$ peak. This is due to the excitation of holes into the $\pi$ band, which will be discussed in Sec. VII.

A further analysis of the angular distribution (Fig. 4) shows that the transient population in the $\pi^*$ band correspond to a localization of the electron population between 0.89 and 1.11 $|\bar{\Gamma}$-$\bar{J}|$ indicating that the $\pi^*$ band is

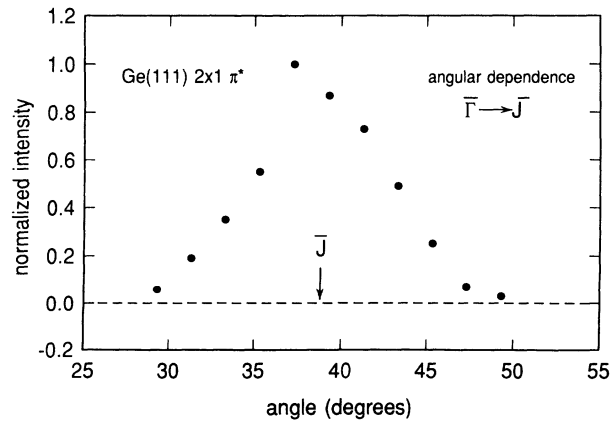


FIG. 4. Normalized $\pi^*$ emission intensity vs emission angle, collected along the [01$\bar{1}$] direction.

positively dispersive along the chain ([01$\bar{1}$]) direction. We have also measured the emission intensity along the $\bar{J}$-$\bar{K}$ direction ([2$\bar{1}$ $\bar{1}$]), which is perpendicular to the chains, and found substantial population along the entire line in the SBZ, consistent with the nearly flat dispersion of the $\pi^*$ band in this direction.[5] Our spectroscopic findings are in good agreement with results from photoemission measurements on heavily doped Ge(111),[4] as well as inverse photoemission,[10] and are consistent with theoretically derived band dispersions.[5]

## IV. DYNAMICS

Inspection of the time-dependent intensities of the $\pi^*$ signal reveals a wealth of information on the surface electron dynamics. All dynamic information is contained in the time-dependent intensities and shapes of the $\pi^*$ peaks collected in photoemission. Measurements were carried out at 300 and 120 K, in an effort to determine the nature of the mechanisms governing the electron dynamics at the surface. Figures 5 and 6 display photoemission spectra collected from the photoexcited Ge surface for different delay times, with substrate temperatures of 120 and 300 K, respectively. In Fig. 5, we note for the early time of 0.3 ps a relatively weak but energetically broad $\pi^*$ peak. Initially, the absorption of the excite pulse at $\Gamma$ creates a dense electron-hole plasma whose bulk densities reach $5\times10^{19}$/cm$^3$ near the surface. $e$-ph scattering, as we will show, drives electrons from the bulk states near the surface into the $\pi^*$ band ~0.4 eV above the $\bar{J}$ minimum (see Fig. 1, bottom). The distribution of hot electrons within the $\pi^*$ band at elevated energies results in the broadened and shifted peak we observe at 0.3 ps. At a later time, as shown with the 5-ps spectrum, the $\pi^*$ peak has grown significantly in intensity. We can conclude that at early times (0.3 ps) the 0.5-eV peak reflects a hot, nondegenerate electron gas, with electrons distributed over a wide energy range but which do not fill all available states, while at 5.0 ps the signal is now indica-

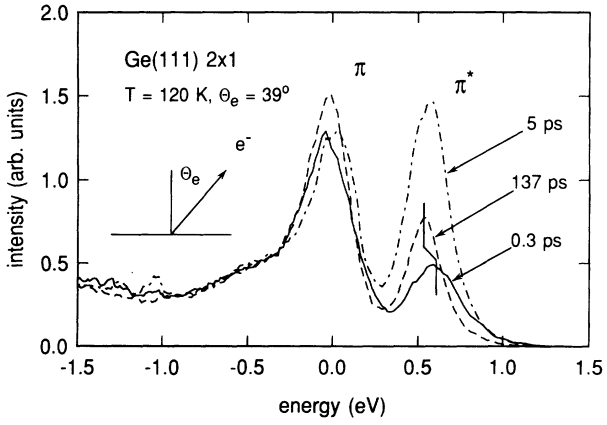


FIG. 5. Photoemission spectra collected at 120 K, and an emission angle of 39° for delay times of 0.3 ps (solid), 5 ps (dot-dashed), and 137 ps (dashed). The energy zero is placed at the peak of the occupied $\pi$ state. (Excitation fluence was ~420 $\mu$J/cm$^2$.)

tive of a cooler, degenerate electron gas. At this time, the intensity of the $\pi^*$ signal exceeds that of the normally occupied $\pi$ signal, i.e, the $\pi$ emission is transiently diminished by a maximum of 10–15%. This effect is due to several possible processes, including scattering of bulk holes into the $\pi$ band created by the excite pulse $\sim$0.4 eV below the VBM (see Fig. 2), weak $\pi$-$\pi^*$ transitions which occur far from the $\bar{J}$ point,[6] and transitions from the $\pi$ state near $\bar{K}$ into the bulk conduction band at $X$. Measurements of the hole dynamics will be discussed in Sec. VII.

At a delay of 5.0 ps, the full width at half maximum (FWHM) of the $\pi^*$ peak in Fig. 5 is 290 meV, nearly 80 meV smaller than at 0.3 ps and the peak has shifted to lower energy by 50 meV, indicating that the entire distribution is relaxing to lower energies. Finally, we note that at the much later time of 137 ps, where we expect the electron temperature to be close to that of the lattice, the signal is both less intense and narrowed (FWHM =220 meV) on both the high- and low-energy sides, resulting in a widened surface band gap relative to that at 5 ps. This transient band-gap change (renormalization) is a density,[11] and hence time-dependent effect which plays an important role in the recombination processes to be described. A detailed investigation of the surface band-gap renormalization is described in Sec. VI.

We can compare the 120-K spectra in Fig. 5 with those collected at 300 K, shown in Fig. 6. We note essentially the same evolution of the peak shapes, i.e., a broadened peak at early time (1 ps), increased peak intensity at 2 ps, and a narrowed and less intense peak at 68 ps. Importantly, for the same excite-pulse fluence, we note that the $\pi^*$ peak intensities are significantly smaller than those collected at 120 K. The smaller intensities are a direct result of the higher $e$-$h$ recombination rates operating at room temperature. At 120 K, the $e$-$h$ recombination rate is significantly reduced, permitting the buildup of electron population in the $\pi^*$ band. We also note that the emission intensity within the surface band gap is higher

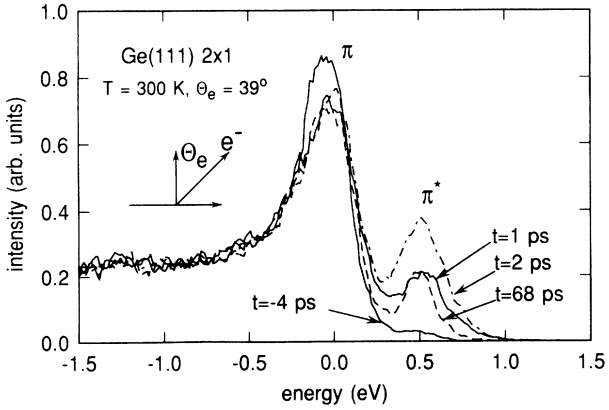


FIG. 6. Photoemission spectra collected at 300 K, and an emission angle of 39° for delay times of −4 ps (solid), 1 ps (solid), 2 ps (dot-dashed), and 68 ps (dashed). The energy zero is placed at the peak of the occupied $\pi$ state. Excitation fluences were $\sim$420 $\mu$J/cm$^2$.

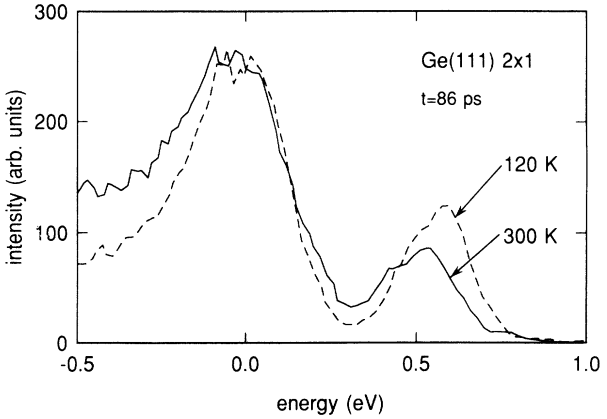


FIG. 7. Comparison of the $\pi$-$\pi^*$ band gap for substrate temperatures of 120 (dashed) and 300 K (solid), at a delay of 86 ps.

for the 300-K spectra than for those collected at 120 K. Figure 7 displays spectra collected at a delay of 86 ps for the two temperatures. The comparison was made at 86 ps in order to allow for equilibration of the electron populations with the lattice. We note that the surface band gap at 120 K is 40 meV wider than at 300 K. The increase observed is in good agreement with temperature-dependent electron-energy-loss-spectroscopy (EELS) studies of the Ge(111)(2×1) surface.[12] As we will discuss, the widening of the surface band gap, and the freezeout of optical phonons at 120 K, strongly affects both the electron dynamics and $e$-$h$ recombination at this surface.

An additional observation concerns the time dependence of the linewidth, shown in Fig. 8 for 120- and 300-K lattice temperatures. We note that for both temperatures, rapid cooling of the electron population occurs within the first 5 ps, followed by a significantly slower narrowing of the linewidth out to the latest delay times studied. While the early time rapid linewidth changes are due to cooling of the electron population, the longer time scale narrowing is due to $e$-$h$ recombination, which

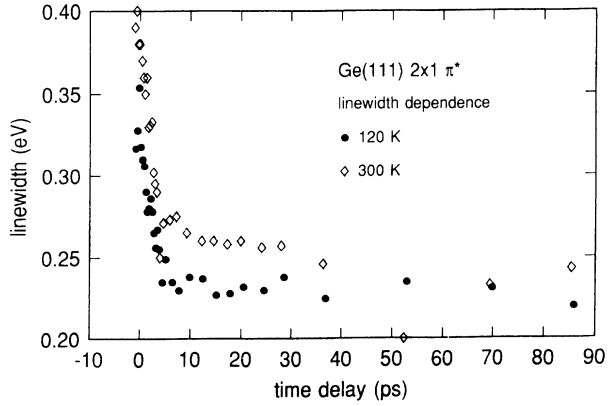


FIG. 8. Linewidth of the $\pi^*$ signal as a function of delay time for120 (filled circles) and 300 K (open diamonds).

lowers the quasi-Fermi level of the $\pi^*$ population. The apparent lattice temperature insensitivity of the intravalley energy-loss rate at early times suggests that low-energy acoustic-phonon emission is the dominant mechanism here. At 120 K, while optical and energetic longitudinal-acoustic-phonon emission and absorption is significantly reduced, the lower-energy acoustic-phonon population is essentially unaffected.

To check that the electrons we observe at the surface did indeed originate from the bulk, we compared $\pi^*$ signal intensities for the excite pulse polarized first parallel and then perpendicular to the chain direction. Optical experiments[6] have shown that perpendicular polarization should result in significantly weaker surface absorption; the signals we measured were unchanged, indicating that the predominant photoexcitation of electrons occurs in the bulk.

In order to monitor the rapid changes in the surface population, we have plotted the normalized $\pi^*$ emission intensity as a function of the delay of the probe relative to the excite pulse (Fig. 9) for lattice temperatures of 120 and 300 K. Only the first 40 ps are displayed, in order to resolve the ultrafast relaxation and recombination processes. In the 300-K scan, we note a rapid increase in intensity near the overlap of the excite and probe pulses, followed by a fast decay within the first 5–7 ps, and finally a slowing of the population loss at later times. The rising edge results from the scattering of bulk electrons into the $\pi^*$ band at $\sim 0.4$ eV above the $\bar{J}$ minimum (see Fig. 1, bottom). The subsequent $\pi^*$ decay suggests a rapid recombination channel which depletes electrons from the surface band. This may be contrasted with the same experiment carried out at 120 K, also shown in Fig. 9. Here the rising edge is not as sharp and the peak in population occurs 2 ps later than for the 300-K scan. After the peak population has been reached, the decay is substantially slower than for the room-temperature case. The strong dependence of the population rise and decay on temperature clearly indicates the involvement of an

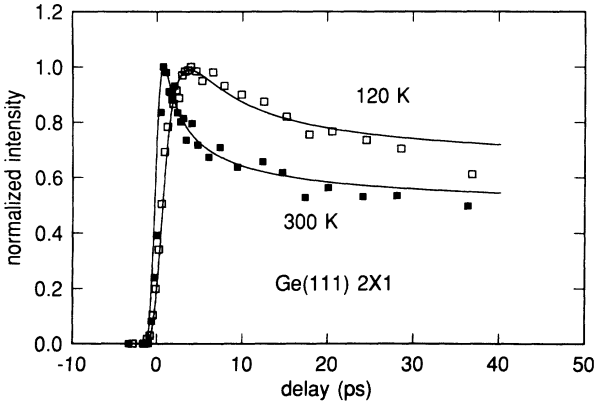


FIG. 9. Normalized $\pi^*$ emission intensity as a function of excite-probe delay time. Filled squares are from spectra collected with the sample at 300 K, while open squares are from the same sample at 120 K. The curves are results from the model calculation fits to the data, as discussed in the text.

$e$-ph scattering mechanism in both the population and eventual decay of electrons in the $\pi^*$ band. Based on the data presented, and our knowledge of the Ge surface and bulk band structure, we propose a model of the surface electron dynamics which involves the coupling of bulk conduction electrons to the surface-$\pi^*$ band by $e$-ph scattering. The excited electron population then rapidly cools to the $\pi^*$ minimum, forming a degenerate electron gas there. The decay of the surface population occurs as $\pi^*$ electrons from the $\bar{J}$ point recombine with holes at the bulk $\Gamma$ point, with the emission of energetic phonons whose energies are on the order of the indirect band gap between these two points (see Fig. 1).

In order to conclude that $e$-ph scattering couples electrons between the surface and bulk as we have described, we must consider all other candidate mechanisms which may be responsible for our observations. Diffusion of electrons into the Ge interior is ruled out, since the $\pi^*$ band is located within the bulk Ge band gap (see Fig. 1). Radiative recombination can be ruled out since this process is independent of lattice temperature. Additionally, photon emission requires nanoseconds or more, and is further inhibited due to the rapid $k$-space separation of electrons and holes (holes are observed to scatter out of the $\pi$ band in less than 7 ps after excitation). This rules out recombination between the $\pi^*$ electrons and $\pi$ holes as contributing significantly to the rapid decay we observe. Auger recombination is also unlikely, since this process requires a carrier density of $\sim 10^{21}/\text{cm}^3$ and, importantly, is lattice temperature independent.[13] We also rule out cleavage-induced defects on the time scale studied here. The overall reproducibility of our results indicates the intrinsic nature of the relaxation and recombination processes we observe. In measurements on the analogous Si surface,[14] defects were invoked to explain the nanosecond time-scale dynamics, and it was shown that the surface defect density affected the $\pi^*$ nanosecond decay rates. We have also carried out experiments on the Si(111)(2×1) surface, in an effort to compare the dynamics of this surface with that of Ge. No significant decay in the Si $\pi^*$ population was observed within the first 100 ps after excitation, in stark comparison with the large population changes we observe for Ge.

A critical difference between the two systems may be found in the energetic location of the surface states within the bulk band gap. For Si, the $\pi^*$ band minimum at $\bar{J}$ is 0.5 eV above the VBM.[15] In Ge, we find this indirect band gap to be $0.13 \pm 0.05$ eV at 300 K, which is in good agreement with both experimental[4,16] and theoretical investigations.[5] Further support for phonon-mediated recombination may be found in electron-energy-loss spectroscopy (EELS) (Ref. 17) and theoretical studies of the surface vibrational spectrum,[18,19] which show the existence of energies (33–40-meV) optical phonons, similar to those in the bulk. In addition, EELS,[12] scanning tunneling microscopy,[20] and optical investigations[6] reveal band-edge broadening ranging from 40–100 meV at 300 K, which effectively reduces the indirect $\pi^*$-VBM band gap even further. This broadening is due to bond-angle fluctuations along the chains, and a small degree of disorder on the surface. Two additional effects also impact the

surface dynamics. As discussed previously, a 40-meV increase in the surface band gap was observed when the sample was cooled to 120 K. The widening of the gap at low temperatures (Fig. 7), in addition to phonon freezeout, as we will discuss, can further inhibit the surface electron population decay. A second consideration involves our observation of surface band-gap renormalization, which narrows the energy difference between the $\pi$ and $\pi^*$ states at high electron densities. The combination of the effects just described results in an indirect $\pi^*$-VBM band gap, comparable to an optical-phonon energy. Such a phonon-assisted recombination process would be exceptionally fast in the case of Ge, which possesses a small indirect $\pi^*$-VBM band gap, and essentially nonexistent in Si, where the indirect gap is significantly larger, in good agreement with our observations.

Importantly, a scattering process mediated by optical phonons should display a dependence upon the lattice temperature. This can be seen by inspection of the $e$-ph deformation-potential scattering rate between valleys $i$ and $j$, given by[21]

$$R(\mathbf{k})=\frac{\pi D_{ij}^2}{\rho_m \omega_{ij}}\{n_{\mathrm{BE}}(\omega_{ij})N(E_k-\Delta E_{ij}+\hbar\omega_{ij}) +[n_{\mathrm{BE}}(\omega_{ij})+1]N(E_k-\Delta E_{ij}-\hbar\omega_{ij})\}\ , \tag{1}$$

where $D_{ij}$ is the deformation-potential constant, $\rho_m$ is the mass density, $\hbar\omega_{ij}$ is the phonon energy, $\Delta E_{ij}$ is the energy difference of the valley minima, and $N(E_k-\Delta_{ij}\pm\hbar\omega_{ij})$ is the final density of states of the band to which the electron scatters. Importantly, the scattering rate is proportional to $n_{\mathrm{BE}}(\omega_{ij})$ when a phonon is absorbed and $n_{\mathrm{BE}}(\omega_{ij})+1$ when a phonon is emitted, where $n_{\mathrm{BE}}(\omega_{ij})=(e^{\hbar\omega_{ij}/k_BT}-1)^{-1}$, the temperature-dependent Bose-Einstein occupation probability. As a consequence, at 120 K the optical-phonon absorption probability is nearly zero, while the probability for emission is reduced to nearly 1 from its 300-K value of 1.35. Hence, phonon scattering from higher-lying bulk states, which feed the $\pi^*$ band, is reduced, delaying the normalized peak intensity to longer times, as we observe. Since, in our model, emission of optical phonons is required to recombine surface electrons and bulk holes, the freezeout of these phonons would slow the rate of decay in the 120-K time scan. This, when combined with the widened indirect band-gap at 120 K, results in the distinct differences observed in Fig. 9. Finally, the leveling out of the decay at longer times is a consequence of the diffusion of bulk holes into the Ge interior. Since the $\pi^*$ electron-valence hole recombination is bimolecular, when the availability of holes at $\Gamma$ is reduced, due to diffusion, we expect the decay rate to slow significantly.

## V. MODEL

The processes described above can be cast in a set of model rate equations which include photoexcitation, bulk electron and hole diffusion, temperature-dependent $e$-ph scattering from the conduction band (CB) into the $\pi^*$ band and $e$-$h$ recombination from the $\pi^*$ minimum to the bulk valence band (VB), mediated by temperature-dependent $e$-ph scattering. The bulk electron and hole diffusion is given by

$$\dot{N}_{e,h}(z,t)=G(z,t)+D_{e,h}\frac{\partial^2 N_{e,h}(z,t)}{\partial z^2}\ , \tag{2}$$

where

$$G(z,t)=\alpha f(1-r)e^{-\alpha z}\frac{1}{2W}\mathrm{sech}^2\left[\frac{t}{W}\right] \tag{3}$$

with boundary conditions imposed by surface scattering

$$\frac{\partial N_e(0,t)}{\partial z}=\frac{\Delta z}{D_e\tau_{\mathrm{CB}-\pi^*}}N_e(0,t) \tag{4}$$

and

$$\frac{\partial N_h(0,t)}{\partial z}=\frac{\Delta z}{D_h\tau_{\pi^*-\mathrm{VB}}}\frac{N_{\pi^*}(t)}{N_{\pi^*}^m}N_h(0,t)\ . \tag{5}$$

The rate of change of the $\pi^*$ population is given by

$$\dot{N}_{\pi^*}(t)=D_e\frac{\partial N_e(0,t)}{\partial z}-D_h\frac{\partial N_h(0,t)}{\partial z}\ . \tag{6}$$

The temperature-dependent scattering and recombination rates are

$$\begin{aligned}\tau_{\mathrm{CB}-\pi^*}^{-1}&\equiv\{\tau_1^{-1}(N_{\mathrm{BE}}+1)\}\ ,\\ \tau_{\pi^*-\mathrm{VB}}^{-1}&\equiv\{\tau_2^{-1}(T)(N_{\mathrm{BE}}+1)\}\ .\end{aligned} \tag{7}$$

$N_e$, $N_h$, and $N_{\pi^*}$ are the bulk electron, hole, and $\pi^*$ electron densities, respectively. $\tau_{1,2}^{-1}$ are the respective $e$-ph scattering rates. $W$ is the laser pulse width, $f=7\times10^{14}/\mathrm{cm}^2$ is the photon flux, $\alpha=9\times10^4/\mathrm{cm}^{-1}$ is the Ge bulk absorption coefficient at 1.76 eV, and $r$ is the surface reflectivity ($\sim30\%$). Equation (2) describes the electron and hole diffusion from the surface after excitation with the excite laser pulse, detailed in Eq. (3). Here the initial spatial density profile is an exponential, which decays with distance from the surface. Equation (4) is a boundary condition at the surface, which includes the scattering of electrons into the $\pi^*$ band. $\Delta z$ is the extinction length of the surface state, which has been set to 5 Å and represents the near-surface region over which an electron can be "trapped" by the $\pi^*$ band. Hence we can interpret $\Delta z/\tau_{\mathrm{CB}-\pi^*}$ as a surface recombination velocity. Equation (5) represents a boundary condition for the holes similar to Eq. (4), with additional considerations. The hole gradient at the surface is modified by the number of $\pi^*$ electrons which, in our model, recombine with holes at $\Gamma$. We therefore include a term, $N_{\pi^*}(t)/N_{\pi^*}^m$, which is the fractional occupancy of the $\pi^*$ band. The product, $N_{\pi^*}(t)N_h(0,t)$, seen in Eq. (5), clearly exhibits the "bimolecular" nature of the recombination. Equation (6) gives the time dependence of the surface population in terms of a difference between electron and hole currents.

Importantly, the rates $\tau_{1,2}^{-1}$ are multiplied by the phonon emission term $N_{\mathrm{BE}}+1$ to include the temperature dependence. The solutions to the coupled rate equations were solved numerically and are shown in Fig. 9. Best

fits to the data were found for diffusion coefficients $D_c = 100$ cm$^2$/sec and $D_h = 10$ cm$^2$/sec and scattering times $\tau_1 = 0.35 \pm 0.05$ ps, $\tau_2(300\text{ K}) = 0.25 \pm 0.05$ ps, and $\tau_2(120\text{ K}) = 1 \pm 0.1$ ps. The significantly longer $\tau_2$ scattering time at 120 K is a direct consequence of the widened indirect band gap at this temperature which, in addition to phonon freezeout, further reduces the $e$-$h$ recombination rate. We point out here that, instead of an ambipolar diffusion coefficient, we have used separate electron and hole diffusion coefficients in the above equations. These coefficients are in reasonable agreement with expectations for values extracted from mobility data for the doping densities present in our samples.[22] This approach approximately accounts for the electrostatic effects due to the time-dependent surface $\pi^*$-electron population. A more involved approach would include the solution of Poisson's equation, but such a treatment would require modeling a modified time-dependent variation of the dielectric constant as an additional parameter, due to the presence of the high-density $e$-$h$ plasma. Instead, the attraction between the $\pi^*$ electrons and bulk holes is accounted for in the hole diffusion coefficient.

We can use the results of the above calculation to determine a surface recombination velocity. The scattering time $\tau_{CB-\pi^*}$ represents the time required to "trap" an electron which has approached the surface to within a distance $\Delta z$. Hence, $\Delta z / \tau_{CB-\pi^*}$ represents a velocity, in this case the surface recombination velocity, which we calculate to be $2.0 \times 10^5$ cm/s at room temperature. This represents a determination of a surface recombination velocity from direct knowledge of the detailed surface scattering and trapping mechanisms. In addition, it is in principle possible to calculate the deformation-potential constant for the scattering processes discussed, from our knowledge of the scattering times. While we estimate values from the above scattering times to be on the order of $\sim 10^8$ eV/cm, an accurate determination would require careful consideration of the dimensional complexities associated with electronic scattering between bulk and surface states.

## VI. BAND-GAP RENORMALIZATION

When a dense electron-hole plasma is formed in a semiconductor, electron-electron interactions lead to a narrowing of the fundamental band gap.[23,24] This renormalization derives from the repulsive nature of electron exchange, due to Pauli exclusion, which leads to a larger average electronic separation and a resultant energy lowering. Renormalization of the fundamental gap is one of a number of important dynamic effects which occur in excited semiconductor systems, and has been studied extensively, and understood quantitatively, in three-dimensional (3D) systems.[11,23–27] More recently, band-gap renormalization has been investigated in two-dimensional (2D) quantum-well systems, where it has been shown that carrier confinement can result in larger absolute band-gap shifts than those observed in 3D plasmas.[28–32] In this section, we will discuss the first investigations of band-gap renormalization in a one-dimensional (1D) system.[33]

Our observations of the surface band-gap renormalization are displayed in Fig. 10, where we observe a significant narrowing of the band gap at early times, corresponding to high electron densities in the $\pi^*$ band. At later times, where the electron density has diminished, a narrowing of the $\pi^*$ emission on both high- and low-energy (band-edge) sides was observed. While the high-energy edge of the $\pi^*$ peak is an indication of cooling of the electron gas and a loss of population, the changes of the low-energy side result from a renormalization of the surface band gap. In order to study this in greater detail, we carried out a series of room-temperature measurements beginning with the most highly excited surface possible. Figure 10 shows a series of spectra collected at various delay times (and hence $\pi^*$ populations) for an excite photon fluence of 780 $\mu$J/cm$^2$. In the region between the $\pi$ and $\pi^*$ peaks (band-gap region), we note, particularly at early times ($t = 2$ ps), the appearance of significant emission intensity. This emission intensity is due to the downward shift of the $\pi^*$ band edge, concomitant with an upward shift of the $\pi$ band edge, i.e., a renormalization of the band edges. In addition, the $\pi$ peak intensity has diminished as a result of the shift of the edge into the gap. At the later time of 11 ps, even though the $\pi^*$ peak amplitude is similar to that at 2 ps, the gap has widened significantly due to a relaxation of the respective band edges toward their unexcited positions. At 68 ps, we observe a continued recovery of the $\pi$ and $\pi^*$ band edges, and the $\pi$ peak intensity. These changes are correlated with a decrease in the electron density within the $\pi^*$ band. The transient changes observed in the time sequence of Fig. 10 represent a renormalization of the surface band gap due to the time-dependent carrier population in the surface band.

A more systematic investigation of the renormalization dependence upon surface carrier density was carried out by analyzing photoemission spectra collected at delays ranging from the earliest after excitation to times in excess of 60 ps. In order to determine the magnitude of the band-gap narrowing with $\pi^*$ electron density, the $\pi^*$

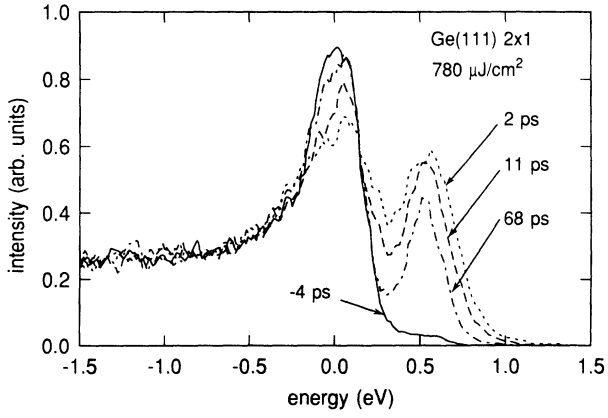


FIG. 10. Photoemission spectra of the Ge(111)(2×1) surface collected at 300 K, and emission angle of 39°, showing the renormalization of the $\pi$-$\pi^*$ band gap. The excitation fluence was 780 $\mu$J/cm$^2$. The energy zero is placed at the peak of the occupied $\pi$ state.

photoemission intensity for various excitation fluences was plotted as a function of delay time. Each data point from this time scan was converted into a $\pi^*$ carrier density. The renormalization of the gap was determined from the corresponding spectrum by fitting Gaussian distributions to the $\pi$ and $\pi^*$ peaks, with emphasis placed upon obtaining good fits to the band edges and emission intensity within the band gap. This fitting procedure was used since the true line shapes are a complicated combination of dynamics and intrinsic broadenings which derive from surface imperfections (disorder and bond-angle fluctuations) along the chain. Three time delay scans corresponding to excitation intensities of 780, 420, and 130 $\mu J/cm^2$ were analyzed in order to study the renormalization over the widest possible dynamic range. The resulting band-gap change as a function of the surface electron density is shown in Fig. 11. For the 780-$\mu J/cm^2$ scan (filled dots), the latest delay times which correspond to the lowest electron densities merge with the open squares which derive from the highest electron density (early time) data points from the 420-$\mu J/cm^2$ scan. The band-gap narrowing determined from the three data sets is plotted in Fig. 11, as a function of electron density along the chains. This was obtained from the division of the surface electron density by the density of surface chains ($1.25\times10^7$/cm). The surface electron density was determined directly from the model calculations discussed in the preceding section. These calculations have indicated that approximately one-third of the electrons excited into the bulk-Ge conduction band at the surface are scattered into the $\pi^*$ surface state. As a check of the simulation, the surface electron density of states near $\bar{J}$ was calculated with an effective mass of $0.28m_e$ derived from inverse photoemission measurements[10] and quasiparticle calculations.[5] Good agreement between the model calculations and this estimate was found. The equivalent surface densities shown in Fig. 11 correspond to $3.5\times10^{11}$–$9\times10^{12}/cm^2$.

At present, we are aware of only one calculation which evaluates the electron exchange energy as it applies to a quasi-1D system, i.e., a quantum wire with cylindrical symmetry.[34] For such equations to be valid, the authors have pointed out that the diameter of the cylinder must be larger than the effective Bohr radius, which is ~30 Å in Ge. Since an estimate of the effective "diameter" for a $\pi$-bonded chain is only ~5 Å, a direct comparison of the theory with our results is difficult. An added complication, not treated in the theory, is the interaction between $\pi^*$ and surface bulk electrons, which may be small due to their rapid diffusion into the crystal. We do wish to point out that, for our densities, a rough agreement is found in the trend of the renormalization with density as well as the absolute magnitude of the effect. It is clear that further understanding of 1D band-gap renormalization will benefit from continued theoretical exploration of wires of smaller lateral dimension.

## VII. HOLE DYNAMICS

Inspection of Fig. 5 reveals a reduction in the amplitude of the $\pi$ peak during and after photoexcitation. Figure 12 displays the time dependence of the $\pi^*$ electron population in the upper frame [12(a)] and the time-dependent change of the $\pi$ peak amplitude in the lower frame [12(b)]. The change in the amplitude was determined by subtraction of individual spectra at a given delay time from a negative time spectrum. The negative time spectrum corresponds to an unexcited surface. The scatter in the data is due to the small changes in the $\pi$ peak amplitude, combined with the subtraction of each spectrum from that collected at negative delay. The eventual recovery of the peak is observed to proceed in

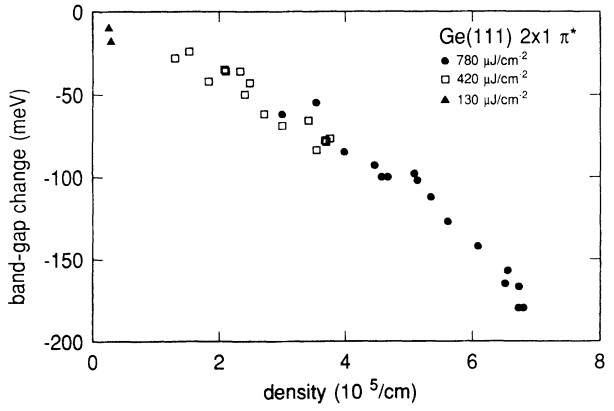


FIG. 11. Plot of the surface band-gap change as a function of the surface electron density, for 1.76-eV excitation intensities of 780 (filled circles), 420 (open squares), and 130 $\mu J/cm^2$ (filled triangles).

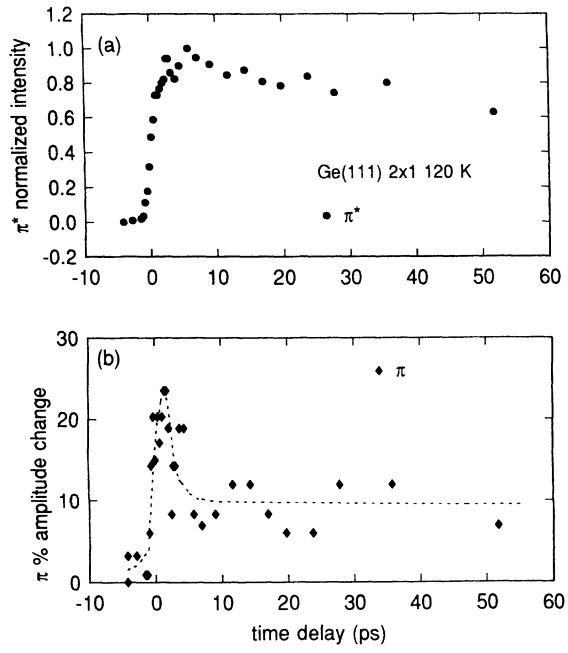


FIG. 12. (a) Normalized $\pi^*$ emission intensity as a function of delay time for a substrate temperature of 120 K. (b) Percent change of the $\pi$ amplitude as a function of delay time. The dashed curve is a guide to the eye.

two steps, indicating two important time scales. At early times, a rapid suppression and recovery of the $\pi$ peak is observed, occurring in a time nearly as short as the duration of the laser pulse. For times greater than 5–7 ps, a much slower change occurs, but the decay rate is more difficult to determine due to the scatter in the data. We can understand the time dependence of Fig. 12(b) in the following manner. The rapid early time behavior is due to the creation of holes in the $\pi$ band at the $\bar{J}$ point. Holes are created directly by excitation of $\pi$ electrons into bulk states. In addition, valence-band holes are created by absorption of the excite pulse, 0.4 eV below the VBM (see Fig. 2). These holes can scatter into the $\pi$ state, analogous to the manner in which electrons scatter from the bulk into the $\pi^*$ band. Since the $\pi$-band maximum is energetically below the VBM, holes will rapidly scatter back to the bulk valence band in an effort to lower their energy. Hole-phonon scattering is extremely rapid,[35] even at 120 K, where the low-energy acoustic-phonon population is unaffected, due to the large valence-band density of states, and as a result we observe the rapid early time behavior shown in Fig. 12(b). The much slower recovery for times greater than 5–7 ps may be due to changes of the band edges associated with the renormalization effects discussed in the preceding section. These affects are density dependent and hence occur over a longer time scale. Since in all experiments described in this paper a 3–8 % reduction in the $\pi$ peak was observed, presumably due to residual gas contamination effects accumulated over the duration of the time scan, we estimate the maximum hole population to be $\sim$10–15 % of the maximum electron population created in the $\pi^*$ band. These observations directly study the ultrafast dynamics of holes at a surface.

## VIII. CONCLUSIONS

Using angle-resolved subpicosecond laser photoemission, we have been able to explore in detail the electron-phonon scattering and energy-loss mechanisms which govern the ultrafast-electron dynamics on the Ge(111)(2×1) $\pi$-bonded surface. Strong temperature-dependent effects observed in the time dependence of the $\pi^*$ population revealed the dominant role played by electron-phonon interactions in coupling bulk and surface electronic states. It was shown that the electron-phonon interaction can drive optically excited bulk electrons into the normally unoccupied $\pi^*$ surface state, $\sim$0.4 eV above the surface band minimum at $\bar{J}$. After rapid cooling of the electron population, recombination of these electrons with bulk valence-bands holes occurs. This recombination rate is strongly reduced when the Ge lattice is cooled to 120 K, and is due to the combination of nearly complete optical-phonon freezeout as well as a 40-meV increase of the surface band gap at this temperature. A model was introduced which incorporated the important scattering and diffusion processes, and fits to the data yielded the relevant scattering times. These times were in turn used to derive a surface recombination velocity directly from our detailed knowledge of the states and scattering mechanisms operating on this surface.

Band-gap renormalization was observed on this surface and the dependence upon density was investigated. Since the surface reconstruction results in the formation of one-dimensional atomic chains and band structure, our investigations study the renormalization effect in a one-dimensional system. Finally, hole dynamics were also investigated, and it was shown that hole residence times in the $\pi$ band were extremely short, consistent with the ultrarapid valence-hole scattering rates. It is thought that the scattering dynamics investigated in this work are representative of, and can be generalized to, a host of other systems, including other similar surfaces, epitaxial heterostructures, and strained-layer superlattices in which electron transport across interfaces is important.

## ACKNOWLEDGMENTS

We wish to thank D. P. DiVincenzo and F. Stern for invaluable discussions concerning this work. In addition, we wish to thank N. Amer and F. J. Himpsel for important discussions. Finally, we thank F. J. Himpsel and E. Haller for providing some of the Ge crystals used in our experiments.

*Present address: Fraunhöfer Institut für Angewandte Festkörperphysik, Tullastrasse 72, D-7800 Freiburg, Federal Republic of Germany.

[1]K. Pandey, Phys. Rev. Lett. **47**, 1913 (1981).
[2]J. Northrup and M. Cohen, Phys. Rev. B **27**, 6553 (1983).
[3]G. Hansson and R. Uhrberg, Surf. Sci. Rep. **188**, 197 (1988).
[4]J. Nicholls, P. Martensson, and G. Hansson, Phys. Rev. Lett. **54**, 2363 (1985).
[5]X. Zhu and S. Louie, Phys. Rev. B **43**, 12 146 (1991).
[6]M. Olmstead and N. Amer, Phys. Rev. B **29**, 7048 (1984).
[7]M. Baeumler and R. Haight, Phys. Rev. Lett. **67**, 1153 (1991).
[8]R. Haight, J. Silberman, and M. Lilie, Rev. Sci. Instrum. **59**, 1941 (1988).
[9]J. Chelikowsky and M. Cohen, Phys. Rev. B **14**, 556 (1976).
[10]J. Nicholls and B. Reihl, Surf. Sci. **218**, 237 (1989).
[11]K Berggren and B. Sernelius, Phys. Rev. B **24**, 1971 (1981).
[12]J. Demuth, R. Imbihl, and W. Thompson, Phys. Rev. B **34**, 1330 (1986).
[13]A. Haug, J. Phys. C **16**, 4159 (1983).
[14]J. Bokor, R. Storz, R. Freeman, and P. Bucksbaum, Phys. Rev. Lett. **57**, 881 (1986).
[15]J. Northrup, M. Hybertsen, and S. Louie, Phys. Rev. Lett. **66**, 500 (1991).
[16]G. Guichar, G. Garry, and C. Sebenne, Surf. Sci. **85**, 326 (1979).
[17]N. DiNardo, J. Demuth, W. Thompson, and P. Avouris, Phys. Rev. B **31**, 4077 (1985).
[18]O. Alerhand and E. Mele, Phys. Rev. B **37**, 2536 (1988).

[19]F. Ancillotto, W. Andreoni, A. Selloni, R. Car, and M. Parrinello, Phys. Rev. Lett. **65**, 3148 (1990).
[20]R. Feenstra, Phys. Rev. B **45**, 7555 (1992).
[21]B. Ridley, *Quantum Processes in Semiconductors* (Oxford University Press, Oxford, 1988).
[22]S. Sze, *Physics of Semiconductor Devices,* 2nd ed. (Wiley, New York, 1981).
[23]W. Brinkman and T. Rice, Phys. Rev. B **7**, 1508 (1975).
[24]J. Inkson, J. Phys. C **9**, 1177 (1976).
[25]D. Ferry, Phys. Rev. B **18**, 7033 (1978).
[26]P. Vashista and R. Kalia, Phys. Rev. B **25**, 6492 (1982).
[27]M. Rinker, H. Kalt, K. Reimann, Y. Lu, and E. Bauser, Phys. Rev. B **42**, 7274 (1990).
[28]G. Trankle, H. Leier, A. Forchel, H. Haug, C. Ell, and G. Weimann, Phys. Rev. Lett. **58**, 419 (1987).
[29]E. Lach, G. Lehr, A. Forchel, K. Ploog, and G. Weinmann, Surf. Sci. **228**, 168 (1990).
[30]S. Schmitt-Rink, C. Ell, S. Koch, H. Schmidt, and H. Haug, Solid State Commun. **52**, 123 (1984).
[31]S. Das Sarma, R. Jalabert, and S. E. Yang, Phys. Rev. B **41**, 8288 (1990).
[32]R. Cingolani, H. Kalt, and K. Ploog, Phys. Rev. B **42**, 7655 (1990).
[33]R. Haight and M. Baeumler (unpublished).
[34]A. Gold and A. Ghazali, Phys. Rev. B **41**, 8318 (1990).
[35]S. Zollner, S. Gopalan, M. Garriga, J. Humlicek, L. Vina, and M. Cardona, Appl. Phys. Lett. **57**, 2838 (1990).